PAPER

Scaling like behaviour of resistivity observed in $LaNiO_3$ thin films grown on $SrTiO_3$ substrate by pulsed laser deposition

To cite this article: S Sergeenkov *et al* 2015 *J. Phys.: Condens. Matter* **27** 485307

IOP Publishing Journal of Physics: Condensed Matter
J. Phys.: Condens. Matter **27** (2015) 485307 (5pp) doi:10.1088/0953-8984/27/48/485307

Scaling like behaviour of resistivity observed in $LaNiO_3$ thin films grown on $SrTiO_3$ substrate by pulsed laser deposition

S Sergeenkov[1,2], L Cichetto Jr[2,3,4], M Zampieri[3], E Longo[3,4] and F M Araújo-Moreira[2]

[1] Departamento de Física, CCEN, Universidade Federal da Paraíba, 58051-970 João Pessoa, PB, Brazil
[2] Departamento de Física, Universidade Federal de São Carlos, 13565-905 São Carlos, SP, Brazil
[3] LIEC: Department of Chemistry, Universidade Federal de São Carlos, 13565-905 São Carlos, SP, Brazil
[4] Institute of Chemistry, Universidade Estadual Paulista: Unesp, 14801-907 Araraquara, SP, Brazil

E-mail: sergei@df.ufscar.br

Received 3 September 2015, revised 18 October 2015
Accepted for publication 29 October 2015
Published 16 November 2015

Abstract

We discuss the origin of the temperature dependence of resistivity ρ observed in highly oriented $LaNiO_3$ thin films grown on $SrTiO_3$ substrate by a pulsed laser deposition technique. All the experimental data are found to collapse into a single universal curve $\rho(T,d) \propto [T/T_{sf}(d)]^{3/2}$ for the entire temperature interval ($20\ \mathrm{K} < T < 300\ \mathrm{K}$) with $T_{sf}(d)$ being the onset temperature for triggering a resonant scattering of conduction electrons by spin fluctuations in $LaNiO_3/SrTiO_3$ heterostructure.

Keywords: nickelates, thin films, resistivity, spin fluctuations, scaling

(Some figures may appear in colour only in the online journal)

1. Introduction

Recently, ferroelectric thin films have rekindled discussion about their potential applications in non-volatile random memory and microsensors devices [1–4]. Of special interest are $LaNiO_3$ (LNO) based materials [5, 6] which exhibit properties quite different from the other members of the nickelates family $RNiO_3$ (R being a rare-earth element). Namely, LNO does not undergo a metal-insulator transition (MIT) from paramagnetic metal to antiferromagnetic insulator. Recall that LNO has the perovskite structure with the pseudo-cubic lattice parameter $a = 0.38$ nm and when it is manufactured in the form of thin films it has a rather good compatibility with oxide substrates typically used for deposition, such as $SrTiO_3$ (STO) and $LaAlO_3$ (LAO), important for applications in ferroelectric FE-RAM.

Based on the substrate properties and intrinsically induced strain in film/substrate heterostructure, it was found [7–10] that magnetic and transport characteristics of deposited LNO films could be drastically changed. More specifically, a partial suppression of the charge ordering (responsible for MIT in nickelates) can be achieved by simply changing the film thickness which leads to formation of a principally new magnetic structure, the so-called pure spin-density wave (SDW) material, exhibiting properties of an antiferromagnetic metal [11–16] (with Neel temperatures $50\ \mathrm{K} < T_N < 100\ \mathrm{K}$). Besides, an important influence of both composition and strain on the electrical properties of LNO thin films has been reported [17].

This work reports on the successful preparation, characterization and transport measurements of highly (l00)-oriented LNO thin films grown on oriented STO substrates by using pulsed laser deposition (PLD) technique. All the obtained resistivity data (as a function of temperature and film thickness) for three different films are found to collapse into a universal curve, exhibiting a scaling like behaviour dominated by conduction electrons scattering on spin fluctuations (supported by formation of SDW within heterostructure interface) for the entire temperature interval.

2. Experimental methods

In order to provide high quality samples (with atomically smooth surfaces compatible with that of the target at a wide range of oxygen pressure), PLD technique was used to deposit thin films of LNO on (1 0 0) oriented STO substrate with typical dimensions of $5 \times 5 \times 0.5$ mm^3. Laser wavelength and repetition rate were $\lambda = 248$ nm (KrF laser with 25 ns pulse duration) and $f = 2$ Hz, respectively. The laser energy was maintained constant during the deposition and the beam was focused on the ceramic targets by a quartz lens to a fluency of around 1.2 J cm^{-2}for all the samples. During ablation, the target was rotated (20 rpm) in order to reduce non uniform erosion and to get the films as homogeneous as possible. The heater power was monitored by a computer during the increase and decrease of the temperature. The temperature during deposition was measured by a thermocouple in contact with the heater and the bottom (back side) of the substrate. The substrate was placed parallel to the target and the distance between them was around 4.8 cm which was the best distance found due to the length of the plume. Before deposition, the base pressure of $P_{\rm base} \leqslant 10^{-7}$ mbar was applied and then the substrates were heated at 800 °C for 20 min to get a carbon free and high crystalline surface. Deposition temperature for all films was defined as $T = 625$ °C under a flowing oxygen pressure of $P_{\rm dep} = 0.22$ mbar maintained by a computerized mass flow controller to 80.0 SCCM (standard cubic centimetres per minute). After the deposition, the samples were *in situ* annealed at the same temperature for 1 h under 500 mbar oxygen pressure to improve the quality of films and decrease the oxygen vacancy. The dense and crack-free LNO ceramic circular target with diameter of 5 cm and thickness of 1.25 cm was prepared from highly pure polymeric precursors by Pechini method [18] using $La_2(CO_3)_3 \times H_2O$ (99.9% Aldrich) and $Ni(OCOCH_3)_2 \times 4H_2O$ (98% Aldrich). Calcination and sintering were performed in the air at 900 °C for 4 h and at 1200 °C for 6 h, respectively. The target was polished after every film deposition to ensure comparable deposition conditions, especially the deposition rate. After that, the pre-ablation process was carried out for 30s to prevent the deposition of the weakly bonded particles.

The electrical resistivity $\rho(T)$ was measured using the conventional four-probe method. To avoid Joule and Peltier effects, a dc current $I = 100$ μA was injected (as a one second pulse) successively on both sides of the sample. The voltage drop V across the sample was measured with high accuracy by a *KT*256 nanovoltmeter.

3. Results and discussion

Microstructure and crystallographic orientation of the films were characterized by x-ray diffraction (XRD) scans. The surface morphology was studied by atomic force microscopy (AFM) and films thickness was confirmed by using field-emission scanning electron microscopy (FEG SEM). Typical XRD spectra and FEG SEM images for the thickest

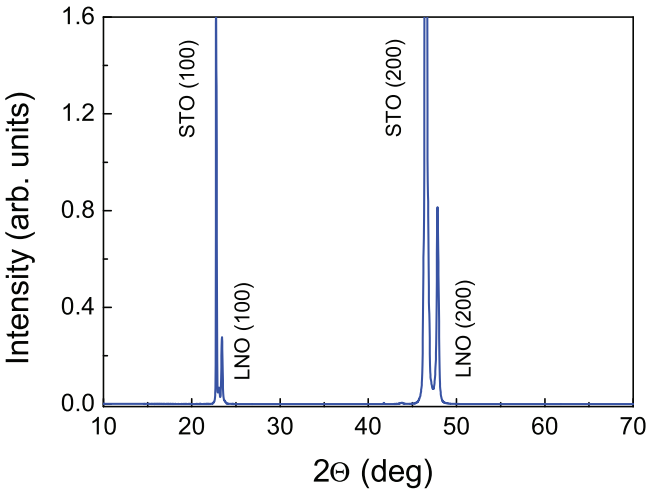

Figure 1. Typical XRD spectrum of LNO films deposited on oriented STO substrate.

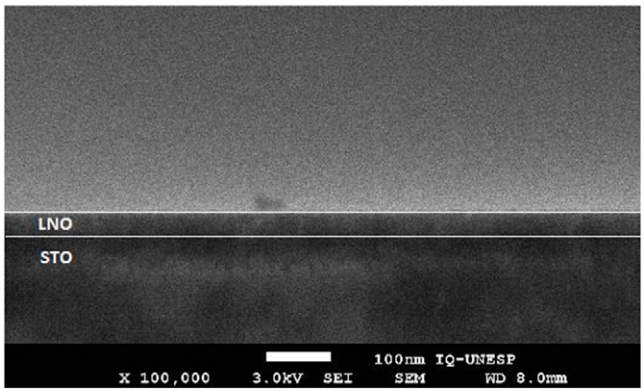

Figure 2. Typical FEG SEM image of LNO films deposited on oriented STO substrate.

LNO films deposited on STO substrate are shown in figures 1 and 2, respectively. AFM scans of LNO/STO hybrid structures (for three LNO films with thickness of $d = 26$ nm, 33 nm, and 46 nm) are depicted in figure 3. Figure 4 shows the deduced from AFM scans relation between film thickness d and the grain size R_g. The results show that for the thinnest films this relation is practically linear. Figure 5 shows the typical results for the temperature dependence of the resistivity $\rho(T)$ in our $LaNiO_3/SrTiO_3$ thin films heterostructure.

Given the above discussion on appearance of magnetic order in LNO/STO hybrid structure, it is quite reasonable to assume that the observed temperature behaviour of resistivity can be attributed to the manifestation of strong long-range spin fluctuations with a characteristic energy $\hbar\omega_{\rm sf} \simeq k_{\rm B}T_{\rm sf}$ corresponding to low-energy spin dynamics spectrum measured by inelastic neutron scattering experiments. It should be pointed out that a rather significant scattering of conduction electrons by spin fluctuations is well documented for many different materials, see, e.g. [19–26] and further references therein. Recently, we suggested a simple phenomenological model based on the resonant like features of SDW type spectrum which result in the observed universal temperature dependence of the resistivity, see [27] for more discussion.

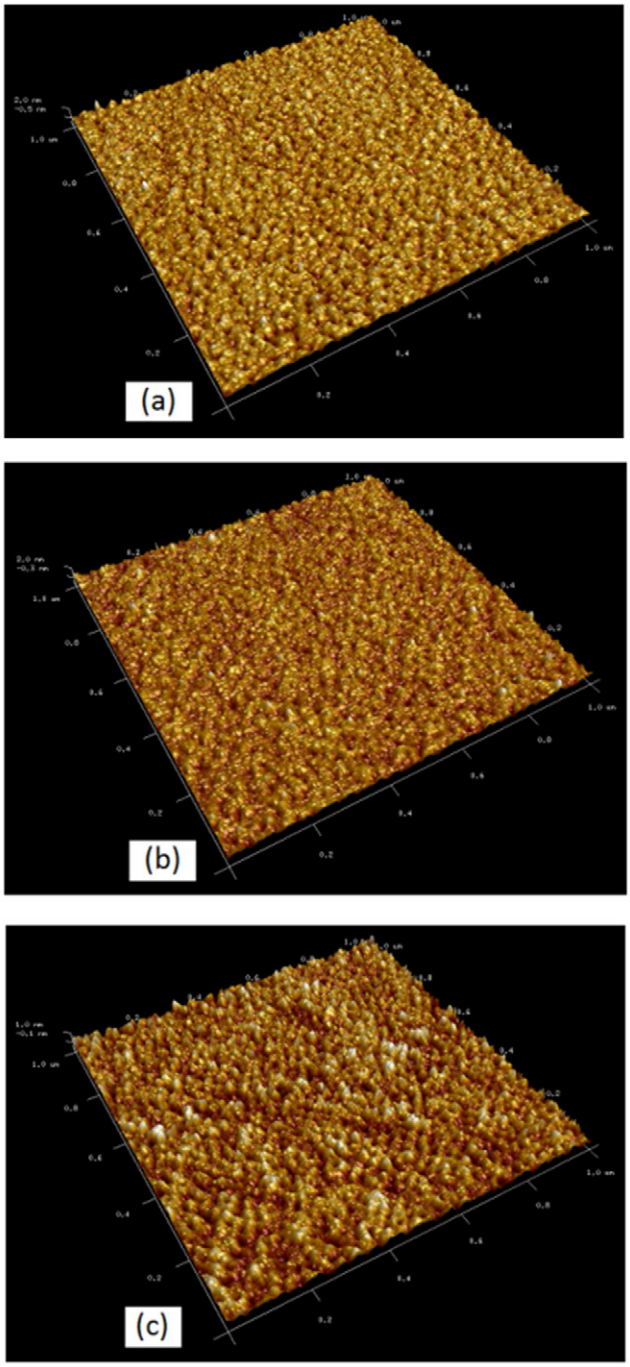

Figure 3. AFM surface scans for LNO films of different thickness d deposited on oriented STO substrate: (a) $d = 26$ nm, (b) $d = 33$ nm, and (c) $d = 46$ nm.

$$\rho(T) = \rho_r + \rho_0\left(\frac{T}{T_{sf}}\right)^{3/2} \tag{1}$$

where ρ_r is the total residual resistivity and T_{sf} is the onset temperature at which spin fluctuations begin to dominate the scattering process in our thin films heterostructure.

Figure 6 shows the best fit of the resistivity data for the thickest film (with $d = 46$ nm) according to equation (1) with $\rho_r = 49$ $\mu\Omega$cm, $\rho_0 = 0.34$ $\mu\Omega$cm and $T_{sf} = 21.5$ K. The latter corresponds to $\hbar\omega_{sf} = k_B T_{sf} \simeq 2$ meV in the inelastic neutron scattering spectrum due to antiferromagnetic spin fluctuations

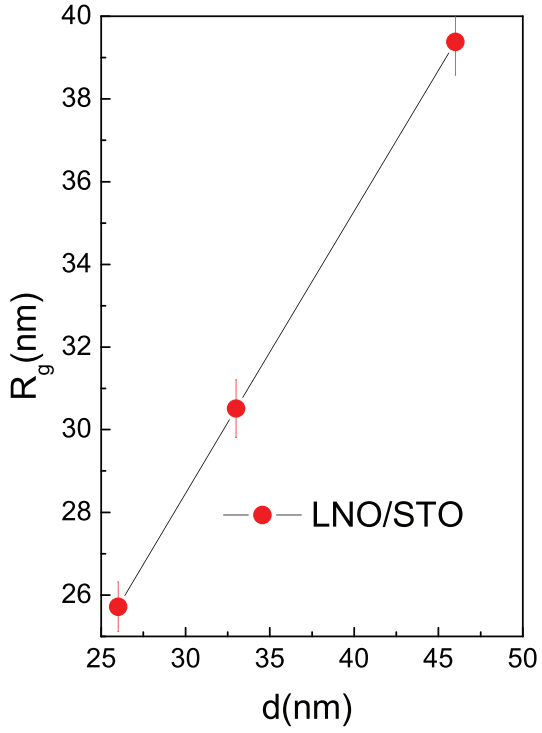

Figure 4. Deduced from AFM scans relation between film thickness d and the grain size R_g.

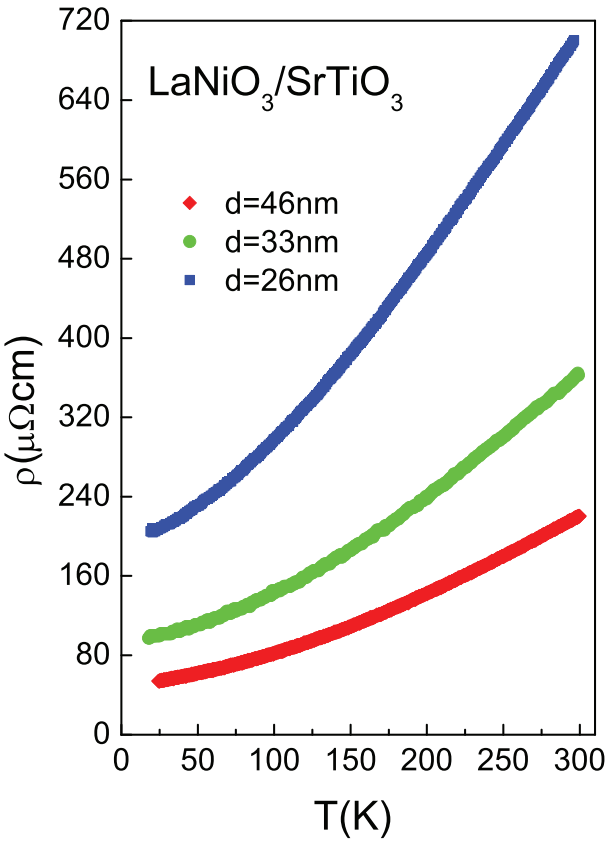

Figure 5. Temperature dependence of the resistivity $\rho(T)$ measured for three LNO thin films deposited on oriented STO substrate.

[21, 27]. Now, using equation (1), we can deduce the dependence of the residual resistivity $\rho_r(d)$ and of the onset spin-fluctuation temperature $T_{sf}(d)$ on film thickness d. The obtained

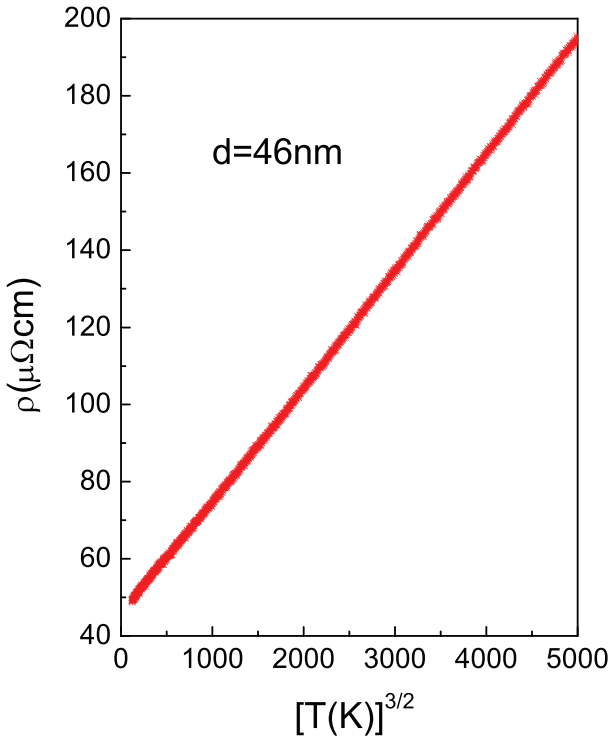

Figure 6. The best fit of the experimental data for the thickest film ($d = 46$ nm) according to equation (1).

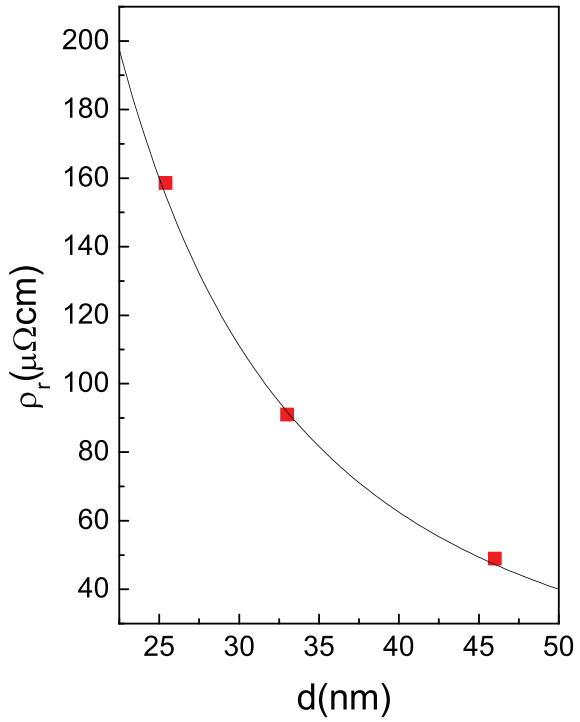

Figure 7. Deduced thickness film d dependence of the residual resistivity $\rho_r(d)$ for three LNO thin films deposited on oriented STO.

results are presented in figures 7 and 8, respectively. Recall that within the free electron gas model, $\rho_r(d)$ is related to the electron density n_e as $\rho_r(d) \propto 1/n_e(d)$. Thus, expectedly, according to figure 7, the electron density increases with increasing the film thickness. On the other hand, according

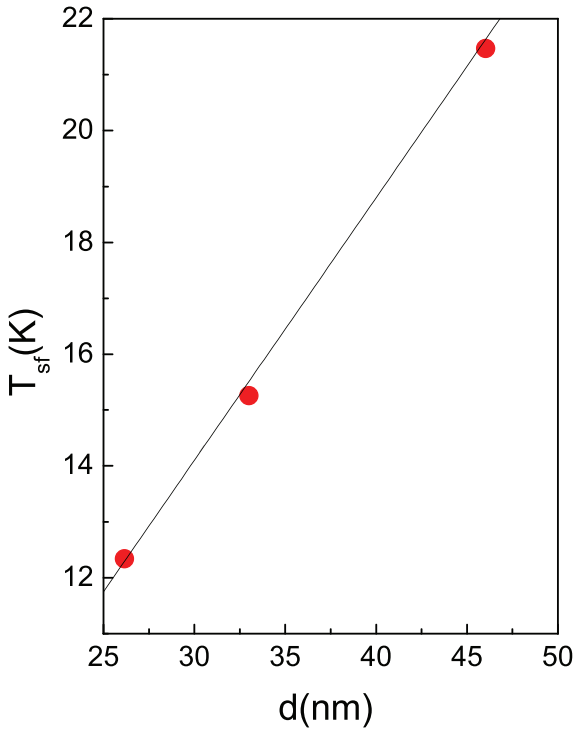

Figure 8. Deduced thickness film d dependence of the onset spin-fluctuation temperature $T_{sf}(d)$ for three LNO thin films deposited on oriented STO.

to figure 8, the thinner is the film, the lower is the spin fluctuations onset temperature triggering the scattering processes in our films. Based on the deduced information about $\rho_r(d)$ and $T_{sf}(d)$, we are able now to fit all the data for all the films by assuming a simple scaling like temperature behaviour of the normalized resistivity $\Delta\rho(T,d)/\rho_r(d)$ as a function of the reduced temperature $T/T_0(d)$ where

$$\Delta\rho(T,d) = \rho(T,d) - \rho_r(d) \tag{2}$$

and

$$T_0(d) = \left[\frac{\rho_r(d)}{\rho_0}\right]^{2/3} T_{sf}(d) \tag{3}$$

Figure 9 is the main result of this paper. As we can see, all the data points (for all temperatures and all films) collapse nicely into a single line fitted (solid line) by equations (1)–(3).

And finally, to justify the universality of the observed $T^{3/2}$ behaviour over the entire measured temperatures, it was suggested [20, 27] that the resonant scattering of conducting electrons by intraband spin fluctuations replenishes the electron distribution (depleted by interband inelastic scattering) while having a little effect on the current, thus making intraband scattering mechanism responsible for the robustness of the $T^{3/2}$ behaviour in intrinsically strained thin films based heterostructure.

4. Conclusion

In summary, by analysing the temperature dependence of the resistivity for three different $LaNiO_3$ thin films grown

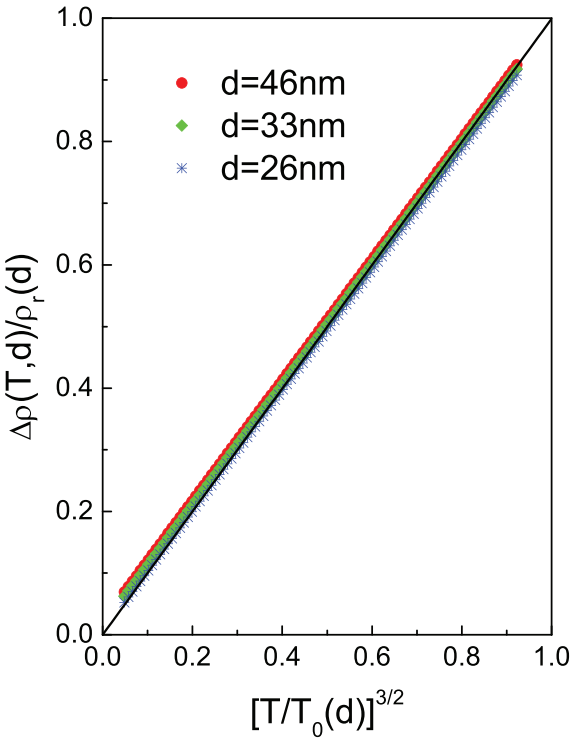

Figure 9. Scaling like behaviour of the normalized resistivity $\Delta\rho(T,d)/\rho_r(d)$ as a function of temperature T and film thickness d for all three films shown in figure 5.

on oriented $SrTiO_3$ substrate (using a pulsed laser deposition technique) we were able to successfully fit all the experimental data by assuming a universal film thickness dependent scaling like law dominated by resonant scattering of conducting electrons on spin fluctuations supported by spin-density wave propagation through the interface boundary of $LaNiO_3/SrTiO_3$ heterostructure.

Acknowledgments

We are very grateful to H Kamimura and R C Gouveia from NanO LaB for their help with resistivity measurements. We would like to thank LMA-IQ for allowing us to use FEG-SEM facilities. This work was financially supported by Brazilian agencies FAPESQ (DCR-PB), FAPESP and CNPq. We are very thankful to FAPESP (CEPID CDMF 2013/07296-2 and 2014/01371-5) for continuous support of our project on nickelates.

References

[1] Ramesh R and Schlom D G 2002 *Science* **296** 1975
[2] Bhardwaj A, Burbure N V and Rohrer G S 2010 *J. Am. Ceram. Soc.* **93** 4129
[3] Fu C *et al* 2010 *J. Electron. Mater.* **39** 258
[4] Liao J *et al* 2012 *Mater. Chem. Phys.* **135** 1030
[5] Ge J *et al* 2013 *Appl. Phys. Lett.* **102** 142905
[6] Pontes D S L, Pontes F M, Pereira-da-Silva Marcelo A, Berengue O M, Chiquito A J and Longo E 2013 *Ceram. Int.* **39** 8025
[7] Freeland J W, Liu J, Kareev M, Gray B, Kim J W, Ryan P, Pentcheva R and Chakhalian J 2011 *Europhys. Lett.* **96** 57004
[8] Han M J, Wang X, Marianetti C A and Millis A J 2011 *Phys. Rev. Lett* **107** 206804
[9] Scherwitzl R, Gariglio S, Gabay M, Zubko P, Gibert M and Triscone J-M 2011 *Phys. Rev. Lett.* **106** 246403
[10] Liu J, Okamoto S, van Veenendaal M, Kareev M, Gray B, Ryan P, Freeland J W and Chakhalian J 2011 *Phys. Rev.* B **83** 161102
[11] Lee S B, Chen R and Balents L 2011 *Phys. Rev. Lett.* **106** 016405
[12] Frano A 2014 *Spin Spirals and Charge Textures in Transition-Metal-Oxide Heterostructures* (Berlin: Springer) chapter 3 (doi: 10.1007/978-3-319-07070-4)
[13] Sakai E, Tamamitsu M, Yoshimatsu K, Okamoto S, Horiba K, Oshima M and Kumigashira H 2013 *Phys. Rev.* B **87** 075132
[14] Zhu M, Komissinskiy P, Radetinac A, Wang Z and Alff L 2015 *J. Appl. Phys.* **117** 155306
[15] Boris A V *et al* 2011 *Science* **332** 937
[16] Detemple E *et al* 2011 *Appl. Phys. Lett.* **99** 211903
[17] Zhu M, Komissinskiy P, Radetinac A, Vafaee M, Wang Z and Alff L 2013 *Appl. Phys. Lett.* **103** 141902
[18] Pechini M 1967 *US Patent* no.3.330.697
[19] Rosch A 2000 *Phys. Rev.* B **62** 4945
[20] Smith M F 2006 *Phys. Rev.* B **74** 172403
[21] Sergeenkov S, Lanfredi A J C and Araujo-Moreira F M 2007 *JETP Lett.* **85** 592
[22] Mansuri I and Varshney D 2012 *J. Alloys Compd.* **513** 256
[23] Choudhary K K 2012 *J. Phys. Chem. Solids* **73** 460
[24] Varshney D, Mansuri I, Shaikh M W and Kuo Y K 2013 *Mater. Res. Bull.* **48** 4606
[25] Choudhary K K 2015 *Int. J. Nanosci.* **14** 1550010
[26] Shaikh M W, Mansuri I, Dar M A and Varshney D 2015 *Mater. Sci. Semicond. Proc.* **35** 10
[27] Sergeenkov S, Cichetto L Jr, Longo E and Araujo-Moreira F M 2015 *JETP Lett.* **102** 383